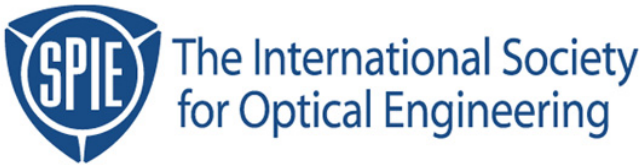

This paper was published in the proceedings of
Optical Microlithography XVI, SPIE Vol. 5040, pp. 1509-1520.
It is made available as an electronic reprint with permission of SPIE.

Process Sensitivity and Optimization with Full and Simplified Resist Models

Mark D. Smith*, Chris A. Mack
KLA-Tencor Corp.

ABSTRACT

While numerical simulation is generally regarded as indispensable for wavefront engineering tasks such as OPC decoration and phase-shift mask design, full resist models are rarely used for this purpose. By "full resist models", we mean models derived from a physical, mechanistic description of the chemical response of the photoresist to exposure and the subsequent PEB and develop processes. More often, simplified models such as an aerial image threshold model or the Lumped Parameter Model (LPM) are used because these models are much faster and make optimization of optical extension technology more tractable.

In a previous study [1], we examined the differences between the process windows calculated with full and simplified models, and we showed that the aerial image threshold model was not capable of describing even the qualitative shape of the process window calculated with the LPM and the full physical models in PROLITH. However, the comparison in our previous study was for an isolated line resist, and this class of resists typically has low contrast in order to improve depth of focus. In the current study, we compare the aerial image threshold model, the aerial image threshold with resist bias model [2], and the Lumped Parameter Model with the full physical models in PROLITH. All of the models are evaluated for simulating the response of both high and low contrast resists, and then we compare the resulting models' ability to predict process windows, line-end shortening, and defect printability.

Keywords: Photoresist modeling, aerial image threshold model, Lumped Parameter Model, LPM, lithography simulation, PROLITH

1. INTRODUCTION

As feature sizes continue to shrink, lithography processes are being pushed to their limits. Technologies that were once considered exotic, such as off axis illumination, phase-shifted reticles, and double exposure processes, are now moving into the mainstream. All of these efforts to implement low k_1 lithography are very engineering intensive, and as a result, numerical simulation is an indispensable tool for wavefront engineering. However, even though many of these techniques concentrate on manipulation of the image projected onto the wafer, the evolution of the modern photoresist has lead to similar gains in resolution as our advances in the optical systems [3], so a complete model for the lithographic process requires both a model for the optical system and a model for the resist.

There are many different photoresist models that have been proposed, and these models range in complexity from very detailed, molecular-level descriptions of the resist to very fast, semi-empirical representations. It is useful to examine a few examples of each of the different types of photoresist models commonly used by lithographers today. Molecular-scale models of the photoresist include dynamic Monte-Carlo [4], molecular dynamics [5,6], and ab initio quantum calculations [7-9]. These models are useful for developing a deeper understanding of resist chemistry and physics from a molecular standpoint, and these models can be used to examine new resist formulations.

Process capability and process optimization studies are usually performed with a model based on a continuum approach, and the examination of various continuum models will be the focus of this paper. We divide continuum models into two broad groups of models: "Simplified" models and "Full Physical" models. The "Simplified" group of models predicts the response of the photoresist directly from the aerial image. These models include the aerial image threshold resist

* mark.d.smith@kla-tencor.com; phone 1-512-381-2318; 8834 North Capital of Texas Highway, Suite 301, Austin, TX 78759

model, the variable threshold resist model [10], and the Lumped Parameter Model [11-14]. The basic philosophy behind the Simplified models is that the model should describe the resist with a minimal number of parameters, and calculations with the model should be very fast. While the model may be physically motivated, the model is not intended to be a mechanistic description of resist response. Simplified models are commonly used for model-based OPC decoration of mask designs, and can provide reasonably accurate results in a short amount of time – full-chip simulations are commonly performed with aerial image threshold models in less than a day. One of the disadvantages of the Simplified models is that the model parameters do not have a physical meaning, so a change in the lithography process will usually require that the model be recalibrated.

An example of a "Full Physical" model is type of model found in PROLITH [15], which is built from continuum, mechanistic models for each step in the lithography process. The philosophy behind these models is that excellent agreement between simulation and experiment can be obtained if each step in the lithography process is described by a detailed, mechanistic model. These models are useful for process optimization. For example, film stack optimization is a very common use case for Full Physical models, because the thin-film interference effects in the stack are modeled in detail. By contrast, a change in the film stack would require that most Simplified models be re-tuned so that they again match experimental results. However, the level of detail and the flexibility of the Full Physical models usually lead to a model with a large number of input parameters, and some of these parameters may be difficult to measure experimentally.

With such a wide variety of models available, each with advantages and disadvantages, one might ask, "Which model is the 'best' model for a photoresist?" The obvious response is given by the famous quote by Albert Einstein: "Things should be as simple as possible, but no simpler." However, the fact that there are so many different models for photoresist demonstrates that "as simple as possible" depends entirely on the task at hand. To compound the issue further, today's task may be different from yesterday's task, warranting a change to a different type of model. For this reason, the goal of the current study is to compare three Simplified models with the Full Physical model in PROLITH, and then determine which models are best suited to different process sensitivity and optimization tasks.

We will investigate three Simplified models in this study. The first model is an aerial image threshold (AIT) model, the second model is aerial image threshold with resist bias (AIT-RB) model, and the third model is the Lumped Parameter Model (LPM). These models are described in detail in Section 2. Our procedure for evaluating the capabilities of the Simplified models for investigating process sensitivity and optimization is very similar to the approach used in our previous paper [1]: The AIT, the AIT-RB, and the LPM will be fit to match the focus-exposure process windows for isolated and dense features calculated with a Full Physical model in PROLITH. Next, the matched Simplified models will be used to predict line-end shortening and defect printability. The predictive capabilities of each Simplified model is then compared with the results from the Full Physical model, which is considered the "correct answer". In Section 3.1, this comparison is performed with a PROLITH model for a high-contrast DUV resist (Sumitomo PEK 130), and in Section 3.2, the comparison is performed with a PROLITH model for a lower-contrast 193 nm resist (Sumitomo PAR 710). Both of these PROLITH models have been carefully tuned to match experimental data. We summarize our results in Section 4.

2. GOVERNING EQUATIONS FOR SIMPLIFIED RESIST MODELS

Both the aerial image threshold (AIT) model and the lumped parameter model (LPM) can be defined in terms of a develop rate equation. For the AIT model, the develop rate for the photoresist is assumed to depend only on the relative intensity of the aerial image at the top of the resist. In addition, the develop rate is a step function of the intensity: if the relative intensity exceeds some threshold value, all of the resist washes away; otherwise, the resist remains on the wafer. Mathematically, the develop rate is described by

$$R(x,y) = \begin{cases} 0, & if \quad I(x,y) < I_{threshold} \\ \infty, & if \quad I(x,y) \geq I_{threshold} \end{cases} \tag{1}$$

where $I(x,y)$ is the aerial image relative intensity at the top of the resist, and $I_{threshold}$ is the aerial image threshold value for conversion of the resist from an insoluble to a soluble film. Optically, the resist is assumed to have the properties of air; that is, an index of refraction of 1.0, and an absorbance of zero. In order to calculate focus-exposure matrices, it is necessary to be able to relate $I_{threshold}$ to the exposure dose. We assume that the aerial image threshold is inversely proportional to the exposure dose, E:

$$I_{threshold} = \frac{E_{threshold}}{E} \tag{2}$$

where $E_{threshold}$ is the only adjustable parameter in the AIT model.

The aerial image threshold with resist bias (AIT-RB) model includes one extra parameter, CD_{bias}, which is simply an offset added to the CD determined by the AIT model. The CD_{bias} parameter accounts for the fact that a real resist does not behave as an ideal switch, and that the PEB and develop processes will lead to a resist bias that is approximately a constant value. Thus, the AIT-RB model has two adjustable parameters: $E_{threshold}$ and CD_{bias}.

For the LPM, the develop rate is assumed to have a power-law dependence on the dose received at each point in the resist. In addition, the image in resist is calculated with a two-step procedure that accounts for physics not included in the AIT model. First, the image in resist is assumed to have the form

$$I(x,y,z) = \left\{ I_0(x,y) + I_1(x,y)\cdot z + I_2(x,y)\cdot z^2 \right\} \cdot \exp\left(-\alpha_{eff}\, z\right) \tag{3}$$

where the first term (in braces) allows the model to account for defocus within the resist film and the second term (the exponential) accounts for absorbance within the film. The parameter α_{eff} is the "effective absorbance", and the photoresist film is assumed to have an "effective thickness", D. Both α_{eff} and D can be used to account for effects not explicitly represented in the model, such as substrate reflectivity and surface inhibition during develop.

The second step in the LPM is to "diffuse" the image in resist with a diffusion length L. Diffusion of the image intensity can be used to account for vibrations during the exposure process, diffusion of photoactive compound during post-exposure bake (PEB), and other effects that decrease image quality [13].

After the image in resist has been calculated, the resist is assumed to dissolve with a develop rate given by

$$R(x,y,z,E) = R_0\left(\frac{E\cdot I(x,y,z)}{E_0}\right)^{\gamma} + R_{\min} \tag{4}$$

where E is the exposure dose, E_0 is the dose-to-clear, γ is the resist contrast, and R_{min} is the minimum develop rate. The parameter R_0 is not an input parameter, but rather is calculated from α_{eff}, D, L, and the other parameters in equation (4). A more detailed description of the LPM is given in reference [14].

3. COMPARISON BETWEEN THE SIMPLIFIED AND FULL RESIST MODELS

We examine two different Full Resist models from PROLITH. The first comparison is with the PROLITH resist model for Sumitomo PEK 130. This is a high-contrast DUV resist that is designed to image semi-dense features. The second comparison is with Sumitomo PAR 710, a 193 nm resist also designed to image semi-dense features. For both resists, similar optical parameters are used: NA = 0.6 with a partial coherence of 0.5. A dimensionless feature size of k1 = 0.4 is chosen, which corresponds to 170 nm lines for DUV and 130 nm lines for 193 nm. The PROLITH models are then used to simulate focus-exposure matrices for semi-dense 1:1.5 lines and isolated 1:9 lines, and this data is used to calibrate the Simplified models. We use the nonlinear least-squares algorithm in the Klarity ProDATA AutoTune™ software package [19,20] to match the Simplified models to the full resist models in PROLITH.

Parameter	Value	Parameter	Value
Dill Parameters		Develop Model	Mack Model
A	0.0	R_{max}	200.0 nm/sec
B	0.320 μm^{-1}	R_{min}	0.08 nm/sec
C	0.03 cm^2/mJ	mth	0.7
PEB Parameters		n	22.3
σ_{RT}	29.3 nm	R_0	0.2
D_{Acid}	3.19 nm^2/sec	δ	200.0 nm
k_{loss}	0.0	t_{dev}	60 sec
k_{quench}	Instantaneous	Film Stack	
Initial Q	0.10	*Resist, thickness*	450 nm
$D_{Quencher}$	0.0	*Resist Refractive Index*	1.71
k_{amp}	0.022 sec^{-1}	*DUV 32, thickness*	60 nm
t_{PEB}	60 sec	*DUV 32,* ***n***	1.595 + 0.555 i
T_{PEB}	110 deg. C		

Table 1: Parameters for the Full Physical model for the DUV Sumitomo resist PEK 130 on a Brewer Science DUV 32 BARC on silicon.

Although designed for the same type of features, PAR 710 is a lower contrast resist than PEK 130. This is mostly due to the fact that the 193 nm resists are not nearly as mature as the DUV resists, which have been widely used for almost 10 years [3]. This is reflected in the model parameters listed in Tables 1 and 2, although this may not be obvious simply by looking at the many parameters listed in the tables. Two contributions to loss of pattern fidelity are diffusion during PEB and a finite develop contrast. Diffusion during PEB can be quantified by examination of the diffusion length during PEB:

$$\sigma_{PEB} = \sqrt{2 D_{acid} t_{bake}} \tag{5}$$

For PEK 130, σ_{PEB} = 19.6 nm, and for PAR 710 σ_{PEB} = 60.7 nm. In addition, the model for PEK 130 includes room temperature diffusion, quantified by the room temperature diffusion length, σ_{RT}. A combined metric for the diffusion can be defined as

Parameter	Value	Parameter	Value
Dill Parameters		Develop Model	Enhanced Mack Model
A	0.0	R_{max}	567.0 nm/sec
B	1.1160 μm^{-1}	R_{min}	0.05 nm/sec
C	0.0214 cm^2/mJ	R_{resin}	567.0 nm/sec
PEB Parameters		n	17.0
σ_{RT}	0.0	l	12.0
D_{Acid}	30.66 nm^2/sec	R_0	0.125
k_{loss}	0.0	δ	220.0 nm
k_{quench}	Instantaneous	t_{dev}	60 sec
Initial Q	0.125	Film Stack	
$D_{Quencher}$	0.0	*Resist, thickness*	350 nm
k_{amp}	0.114 sec^{-1}	*Resist Refractive Index*	1.699
t_{PEB}	60 sec	*AR19, thickness*	85 nm
T_{PEB}	130 deg. C	*AR19,* ***n***	1.73 + 0.395 i

Table 2: Parameters for the Full Physical model for the 193nm Sumitomo resist PAR 710 on Shipley AR19 on silicon.

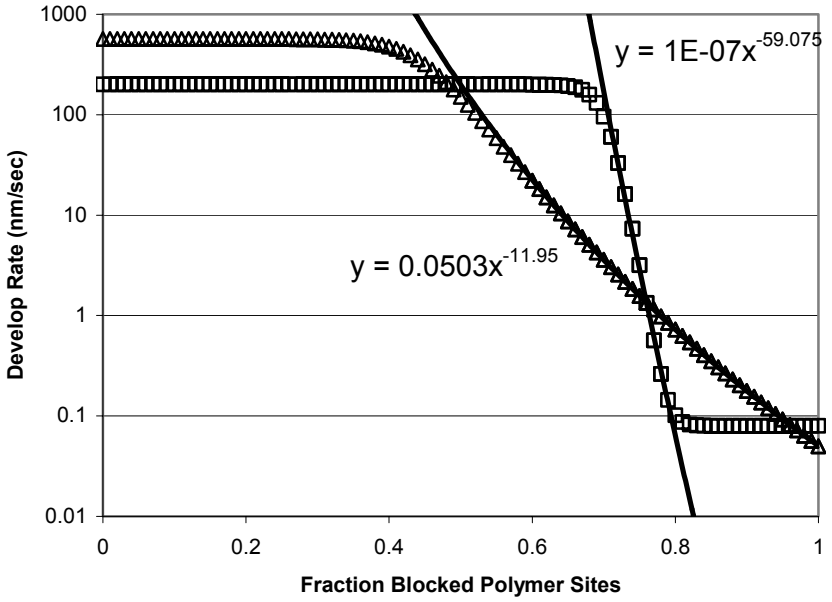

Figure 1: Develop rate curves for the PROLITH Full Resist model for Sumitomo PEK130 (squares) and for Sumitomo PAR 710 (triangles). The solid curves represent power-law fits to the develop rate. The equations for these fits are also shown on the graph.

$$\sigma_{total} = \sqrt{\sigma_{RT}^{\ 2} + \sigma_{PEB}^{\ 2}} \qquad (6)$$

Thus, the overall diffusion length for PEK 130 is 35.3 nm, while the overall diffusion length for PAR 710 is almost twice as large, 60.7 nm. This indicates that the PEB process for PAR 710 will decrease pattern fidelity more than the PEB process for PEK 130.

PAR 710 and PEK 130 also have dramatically different develop rate responses, as shown in Figure 1. The develop contrast contribution to the overall resist contrast can be quantified by fitting a power-law expression to the curves in the figure with the form

$$R = R_o m^a \qquad (7)$$

where m is the fraction of blocked polymer sites. A power-law fit to the develop rate for PEK 130 gives a = -60, and a fit to PAR 710 gives a = -12. Thus, PEK 130 responds more like an ideal, infinite-contrast solubility switch. From this cursory analysis, we find that both the PEB and develop processes are lower contrast for PAR 710 than for PEK 130.

3.1 Comparison of the Simplified models with the PROLITH model for PEK 130

As described at the beginning of this section, focus-exposure matrices are calculated for 170nm lines on a dense pitch (425nm) and on an isolated pitch (1700nm). A nonlinear least-squares calculation led to the parameters listed in Table 3 for the Simplified resist models. In Figure 2 is a comparison between the process windows for the dense features for all of the models. As shown in the figure, the AIT model has an incorrect dose-to-size for features at best focus. This is likely due to the least-square algorithm fitting the features at extreme values of focus. The AIT-RB and the LPM models both reproduce the correct general shape and position of the process window, when compared with the process window for the Full resist model for PEK 130.

Shown in Figure 3 are the results for the isolated features. Again, we find that the AIT model has the incorrect shape, and the incorrect dose-to-size for the features at best focus. The AIT-RB model also appears to have problems – the fit for the dense features is much better for the AIT-RB model. This indicates that this model does not correctly predict the iso-dense bias for PEK 130. The LPM appears to give a satisfactory fit to the process window for both the isolated and dense features.

Next, we examine the ability of the Simplified models to predict line-end shortening. For this test, we start with a tee-shaped pattern with 170 nm lines and then we measure the gap-width in the resist as we change the gap-width on the mask, as shown in Figure 4. The error in the calculation is defined as the percent error between each Simplified model and the Full resist model, and as shown in Figure 5, the AIT model does not predict the gap-width well for small gap-widths on the mask. The other models predict smaller feature sizes than the AIT for gaps smaller than 200nm. This is in agreement with the predictions by the Full resist model in PROLITH.

The final test for the DUV resist models is a defect printability test. Here we place a 50 nm square of chrome exactly in the middle of the gap in the line-end shortening mask. For this test, we examine 170 nm lines with a 170 nm gap. Listed in Table 4 are the predicted resist CDs with and without the chrome defect, along with the predicted change in CD by addition of the defect – this method of analyzing the results emulates a die-to-die reticle inspection. As demonstrated in the table, all of the Simplified models accurately calculate the change in the CD, but only the LPM correctly predicts the gap CD with and without the defect.

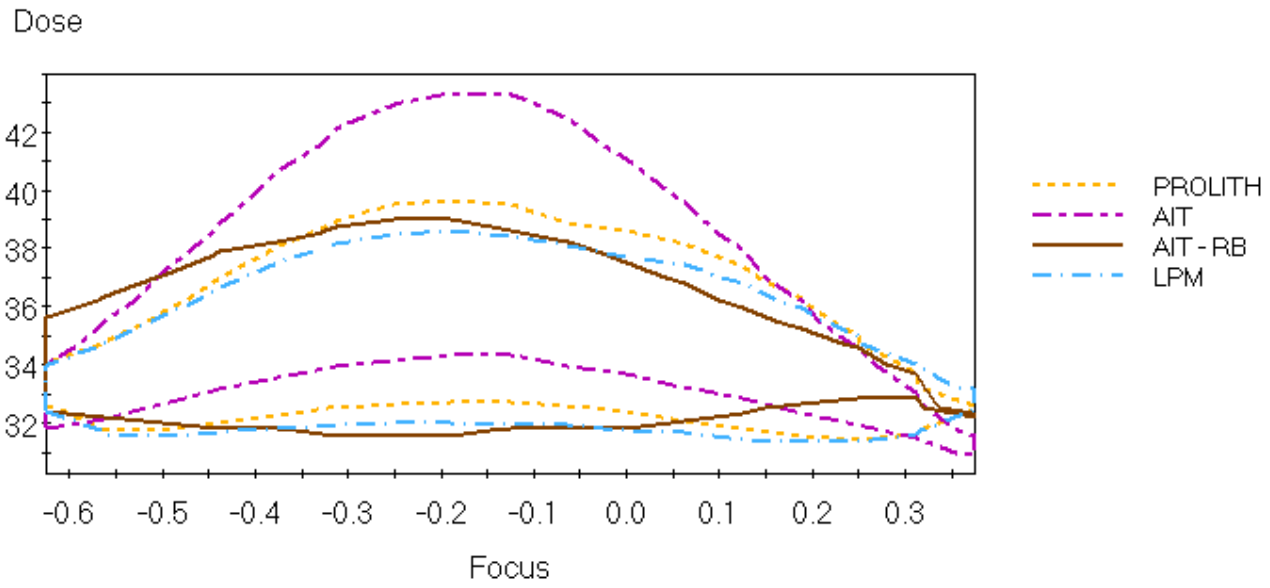

Figure 2: Process window for dense 170 nm lines on a 425 nm pitch calculated with the Full resist model for PEK 130. Also shown are the process windows for the Simplified models that were matched to the Full PROLITH model.

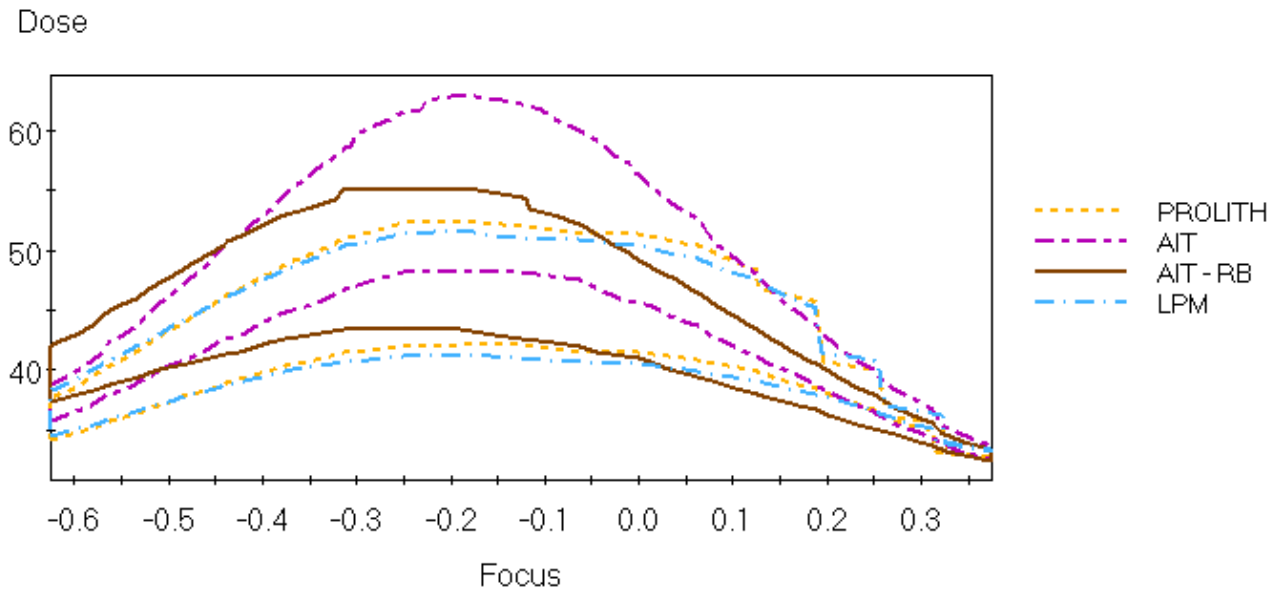

Figure 3: Process window for isolated 170 nm lines on a 1700 nm pitch calculated with the Full resist model for PEK 130. Also shown are the process windows for the Simplified models that were matched to the Full PROLITH model.

Model Parameter	**Match to PEK 130**	**Match to PAR 710**
AIT Model		
$E_{threshold}$	12.4 mJ/cm^2	8.7 mJ/cm^2
Goodness of Fit (σ)	15.4 nm	43.3 nm
AIT-RB Model		
$E_{threshold}$	13.5 mJ/cm^2	12.0 mJ/cm^2
CD_{bias}	-26.4 nm	-54.8 nm
Goodness of Fit (σ)	16.7 nm	14.4 nm
LPM		
Effective Absorbance (α)	0.058 um^{-1}	0.787 um^{-1}
Resist contrast (γ)	28.19	10.91
Dose-to-Clear (E_o)	14.0 mJ/cm^2	12.3 mJ/cm^2
Aerial image diffusion length	37.5 nm	40.0 nm
Goodness of Fit (σ)	3.9 nm	7.0 nm

Table 3: Parameters for the Simplified Resist models resulting from the least-squares fit to simulated focus-exposure data for PEK 130 and PAR 710. Also listed in the table is the goodness of fit parameter, s, which is the root-mean-square of the difference between the CD calculated with the Simplified model and the Full PROLITH model.

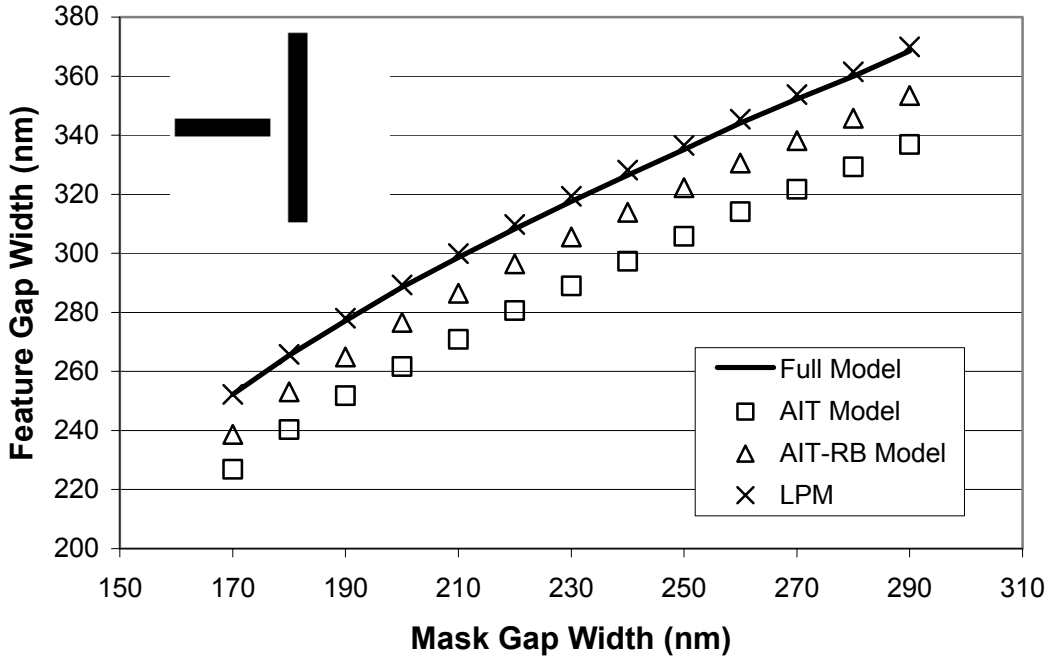

Figure 4: Predicted line-end shortening for the 170 nm tee pattern shown at the top of the graph for Full and Simplified models for PEK 130.

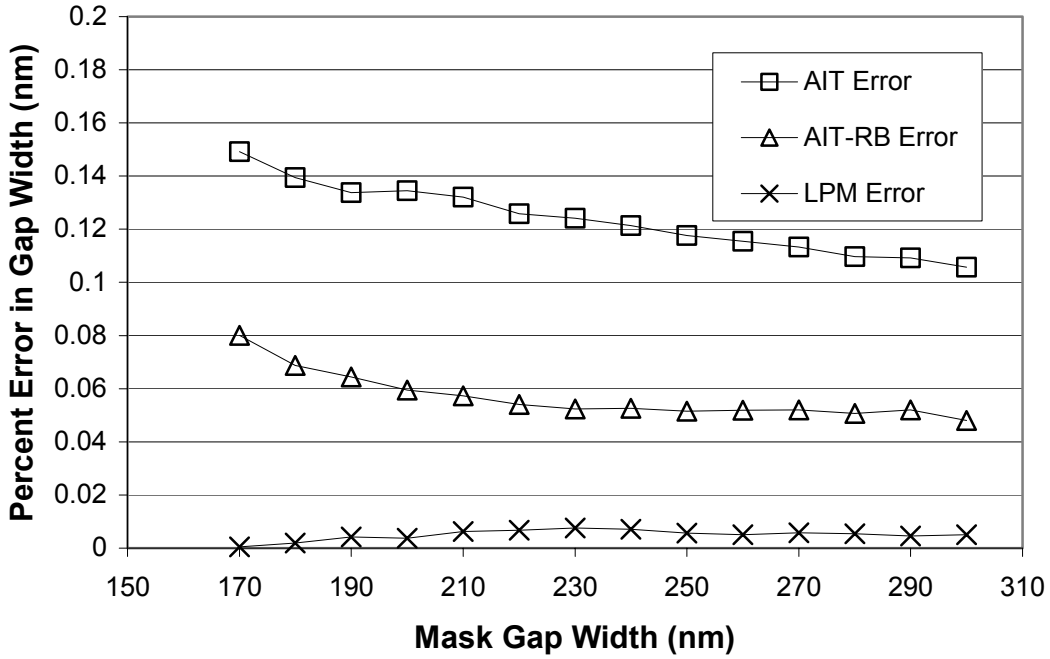

Figure 5: Error in the gap width predicted by the Simplified models when compared with the predictions of the Full Resist model for PEK 130 in PROLITH.

	CD without Defect	CD with Defect	Change in Gap CD
Full Model	252.3	228.3	24.0
AIT Model	226.9	203.1	23.8
AIT-RB Model	238.7	212.1	26.6
LPM	252.2	230.1	22.1

Table 4: Gap width in the 170nm line end shortening tee pattern for the Full model for PEK 130 in PROLITH and for the Simplified models matched to the Full PROLITH model. Results are given for the original mask, and for the mask with a 50nm square chrome defect in the middle of the gap. Examination of the change in gap CD is similar to a die-to-die comparison.

3.2 Comparison of the Simplified models with the PROLITH model for PAR 710

As for the DUV resist, Simplified resist models for the 193 nm system are trained to match focus-exposure matrices calculated with the PROLITH Full resist model for PAR 710 for dense and isolated lines. Here we image 130 nm lines, which correspond to $k_1 = 0.4$. This is the same k_1 as for the DUV resist models. The results of the AutoTune calibration are reported in Table 3, and process windows for the dense and isolated features are shown in Figures 6 and 7. As shown in the figures, the AIT model does not predict the dose-to-size correctly or the general shape of the process window. Both the AIT-RB and the LPM show better agreement with the Full resist model for PAR 710.

For the line-end shortening test, we examine 130 nm lines in a tee-pattern, and we again vary the gap. As shown in Figures 8 and 9, the AIT-RB and LPM models show much smaller errors that the AIT model. Just as was demonstrated for the DUV resist, the AIT model does not predict that the gap is starting to scum, while the other Simplified models correctly predict this behavior for small gaps.

In the defect printability test, we examine a 130 nm tee-pattern with a 140 nm gap, and we place a 40nm square of chrome in the gap. As shown in Table 5, only the LPM predicts the change in CD within 20% of the value predicted by the Full model. As in the DUV test, the AIT model predicts that the gap width is too large, both with and without the defect. The change in CD is also predicted to be about one-third the size of the change calculated with the Full resist model. This result is not surprising, when you consider that the PAR 710 Full Resist model has a relatively low contrast, and the AIT model is effectively an "infinite contrast" model. The AIT-RB model over-predicts the impact of the defect on the gap CD. The Simplified model that gives the best results is the LPM. Even though the LPM does not give perfect results (it under-predicts the change in CD by 12nm), it does not suffer the catastrophic failures of the AIT and the AIT-RB models.

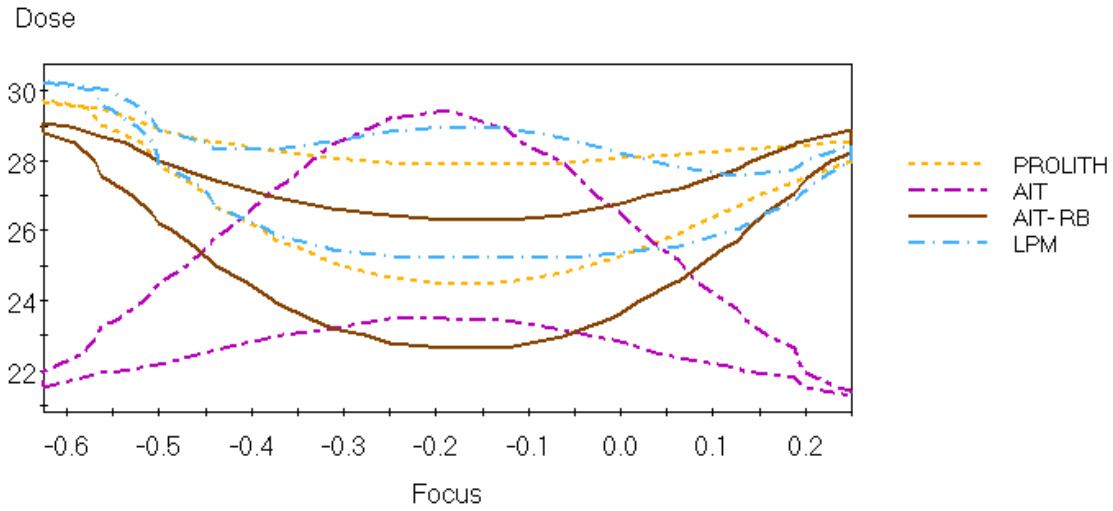

Figure 6: Process window for dense 130 nm lines on a 325 nm pitch calculated with the Full resist model for PAR 710. Also shown are the process windows for the Simplified models that were matched to the Full PROLITH model.

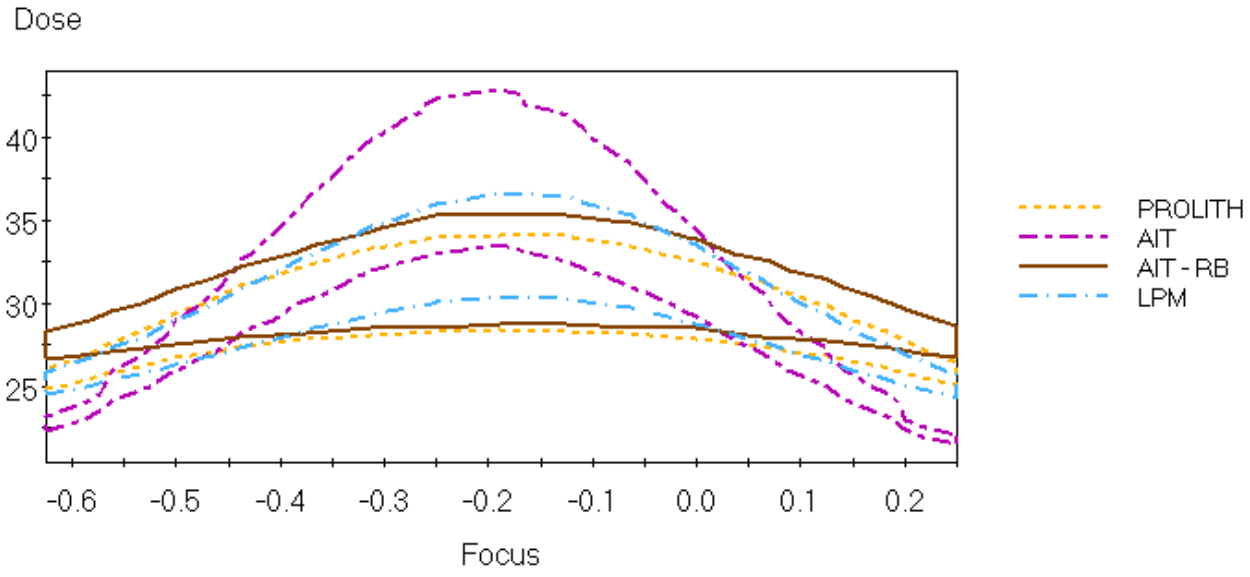

Figure 7: Process window for isolated 130 nm lines on a 1300 nm pitch calculated with the Full resist model for PAR 710. Also shown are the process windows for the Simplified models that were matched to the Full PROLITH model.

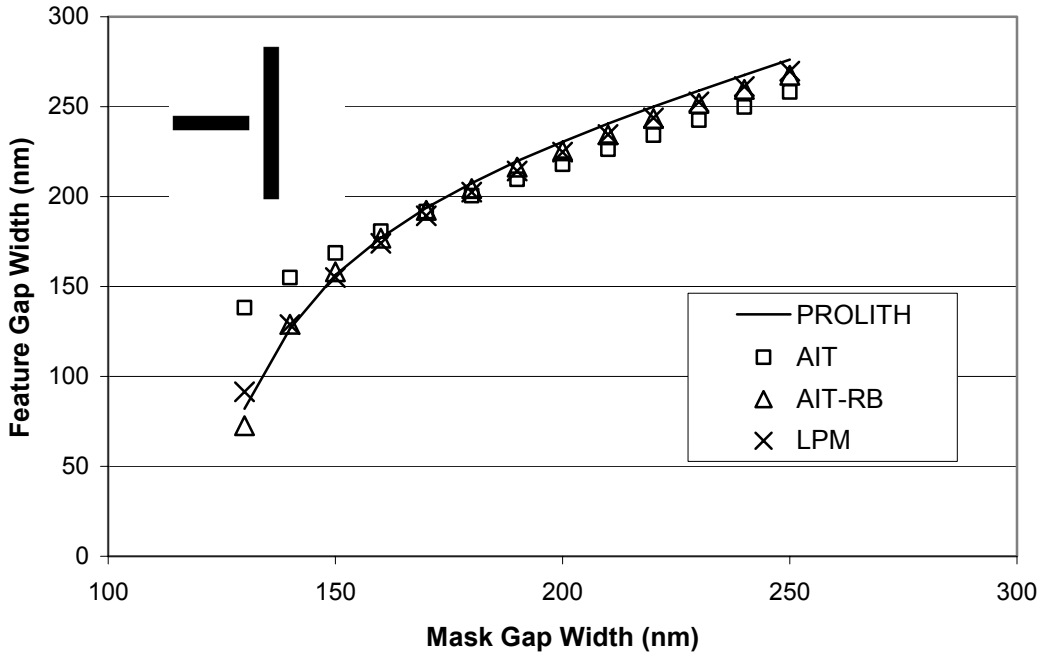

Figure 8: Predicted line-end shortening for a 130 nm tee pattern shown at the top of the graph for Full and Simplified models for PAR 710.

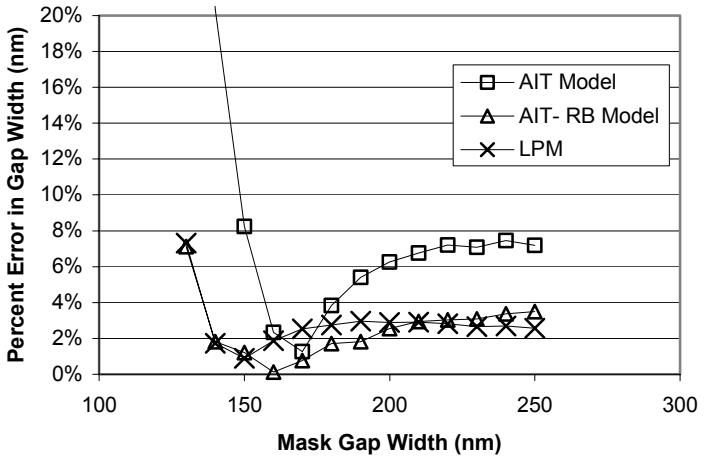

Figure 9: Error in the gap width predicted by the Simplified models when compared with the predictions of the Full Resist model for PAR 710 in PROLITH.

4. SUMMARY AND CONCLUSIONS

In this study, we have examined matching Simplified models such as the AIT model, the AIT-RB model, and the LPM to results calculated with the Full Physical model in PROLITH. On the whole, the higher-contrast, DUV resist was much easier to match than the lower-contrast, 193 nm resist. This is not surprising, especially for the aerial image models, which are "infinite contrast" models. The addition of a resist bias appears to improve the aerial image threshold model, especially for the prediction of process windows. The resist bias concept also appears to dramatically improve the prediction of line-end shortening for both the DUV and the 193 nm resists. Considering that the resist bias is a relatively simple concept, and only one additional parameter compared with the AIT model, the results with AIT-RB are surprisingly good.

The AIT-RB model does not predict the 193nm defect printability results as well as the LPM. The performance of the LPM can be attributed to the inclusion of aerial image diffusion, which mimics image degradation during PEB, and the inclusion of a finite resist contrast. These are the two physical phenomena we examined when comparing the contrast of the models for PEK 130 and PAR 710. In the study by Fuard et al [21], it was found that the addition of aerial image diffusion gave much better results than a simple threshold model. The LPM is the next logical step to improve these models: with only two additional parameters, the LPM includes the physics of absorbance and finite develop rate contrast. Looking to the future, the absorbance of the film may be critical for 157nm, where the resist absorbance is high. For this case, the advantages of the LPM over the other simplified models in this study may be even more dramatic.

	CD without Defect	CD with Defect	Change in Gap CD
Full Model	126.5	64.0	62.5
AIT Model	155.0	131.6	23.4
AIT-RB Model	129.0	Scum	129.0
LPM	128.9	78.0	50.9

Table 5: Gap width in the line end shortening tee pattern with 130nm lines and a 140nm gap. Calculations are performed with the Full model for PAR 710 in PROLITH and with the Simplified models matched to the Full PROLITH model. Results are given for the original mask, and for the mask with a 40nm square chrome defect in the middle of the gap. Examination of the change in gap CD is similar to a die-to-die comparison.

5. REFERENCES

1. M.D. Smith, J.D. Byers, and C.A. Mack, "A comparison between the process windows calculated with full and simplified resist models", *Proc. SPIE* **4691** (2002) pp 1199-1210.
2. J.S. Petersen, *Extending Semiconductor Lithography Resolution using Image Process Integration, Course Notes* from Petersen Advanced Lithography (PAL), Austin, TX.
3. R.R. Dammel, "Polymers for Lithography, or The Red Queen's Race", *Proc. SPIE*, Vol. 4690 (2002) pp. 1-10.
4. G.M. Schmid, S.D. Burns, M.D. Stewart, C. Willson, "Mesoscale simulation of the lithographic process", *Proc. SPIE*, Vol. 4690 (2002) pp 381-390.
5. M. Toriumi, T. Ohfuji, M. Endo, H. Morimoto, "Analysis of molecular diffusion in resist polymer films simulated by molecular dynamics", *Proc. SPIE,* Vol 3678 (1999) pp 368-379.
6. M. Toriumi, I. Okabe, T. Ohfuji, M. Endo, H. Morimoto, "Temperature dependence of acid molecular diffusion in resist polymer films simulated by molecular dynamics", *Proc. SPIE,* Vol 3999 (2000) pp. 1056-1061.
7. NN. Matsuzawa, H. Oizumi, S. Mori, S. Irie, E. Yano, S. Okazaki, A. Ishitani, "Theoretical estimation of absorption coefficients of various polymers at 13nm", *J. Photopolym. Sci. Tech.*, Vol. 12 (1999) pp 571-576.
8. N.N. Matsuzawa, H. Oizumi, S. Mori, S. Irie, S. Shirayone, E. Yano, S. Okazaki, A. Ishitani, D.A. Dixon, "Theoretical calculation of photoabsorption of various polymers in the extreme ultraviolet region", *Jpn. J. Appl. Phys.,* Vol. 38 (1999), pp 7109-7113.
9. N.N. Matsuzawa, S. Mori, E. Yano, S. Okazaki, A. Ishitani, D.A. Dixon, "Theoretical calculations of photoabsorption of molecules in the vacuum ultraviolet region", *Proc. SPIE*, Vol. 3999 (2000), pp 375-384.
10. Y. Granik, N. Cobb, T. Do, "Universal Process Modeling with VTRE for OPC", *Proc. SPIE*, Vol 4691 (2002).
11. R. Hershel, C.A. Mack, "Lumped parameter model for optical lithography," Chapter 2, *Lithography for VLSI, VLSI Electronics – Microstructure Science*, R. K. Watts and N.G. Einspruch, eds., Academic Press (New York:1987), pp 19-55.
12. C.A. Mack, "Enhanced lumped parameter model for photolithography", *Proc. SPIE*, Vol. 2197 (1994) pp. 501-510.
13. T.A. Brunner, R.A. Ferguson, "Approximate models for resist processing effects", *Proc. SPIE*, Vol. 2726 (1996) pp. 198-207.
14. J. Byers, M.D. Smith, C.A. Mack, "3D lumped parameter model for lithographic simulations", *Proc. SPIE*, Vol. 4691 (2002).
15. C.A. Mack, *Inside PROLITH: A Comprehensive Guide to Optical Lithography Simulation*, FINLE Technologies, (Austin, TX: 1997)
16. C.A. Mack, "New kinetic model for resist dissolution", *J. Electrochem. Soc.*, Vol. 139 (1992) pp. L35-L37.
17. C.A. Mack, "Absorption and reflectivity: designing the right photoresist", *Microlithography World* (Spring 1999).
18. M.D. Smith, C.A. Mack, "Examination of a simplified reaction-diffusion model for post-exposure bake of chemically amplified resists", *Proc. SPIE*, Vol. 4345 (2001) pp. 1022-1036.
19. S. Jug, R. Huang, J.D. Byers, C.A. Mack, "Automatic calibration of lithography simulation parameters", *Proc. SPIE*, Vol. 4404 (2001) pp. 380-395.
20. J. Byers, C. Mack, R. Huang, S. Jug, "Automatic calibration of lithography simulation parameters using multiple data sets", *Proc. Micro and Nano-Engineering* (2002).
21. D. Fuard, M. Besacier, P. Schiavone, "Assessment of different simplified resist models", Proc. SPIE, Vol. 4691 (2002) pp. 1266-1277.